Mathematical Models of Nonlinear Effects in Asymmetric Catalysis: New Insights Based on the Role of Reaction Rate

Donna G. Blackmond*

Contribution from the Max-Planck-Institut für Kohlenforschung, D-45470 Mülheim-Ruhr, Germany

Received August 29, 1997[⊗]

Abstract: This work demonstrates how the mathematical models developed by Kagan and co-workers[1a,b] to describe nonlinear enantioselectivity behavior may also be used to predict reaction rate as a function of catalyst enantiomeric excess in asymmetric catalytic reactions. Comparison of these predictions with experimental reaction rate measurements may thus be used to provide an independent confirmation of the model. The predictions of reaction rate reveal striking consequences for nonlinear catalytic behavior. A strong amplification in product chirality may come at the cost of a severely suppressed rate of product formation; in comparison, a system exhibiting a *negative* nonlinear effect in product enantioselectivity can provide a significantly *amplified* rate of formation of the desired product. Consideration of the kinetic behavior of these systems can provide valuable mechanistic insights and may help in the development of efficient synthetic strategies using nonenantiopure catalyst mixtures.

Introduction

Asymmetric catalytic synthesis of enantiomerically enriched products has become an important tool in practical organic synthesis. An interesting feature of these reactions which has been highlighted in the recent literature is the observation in certain cases of a nonlinear correlation between the enantiomeric excess of the reaction product and that of the chiral catalyst or auxiliary.[1,2] Kagan and co-workers reported the first examples of such nonlinear effects more than a decade ago, and they developed mathematical models to describe this behavior. The results from such modeling have been used to provide insights about reaction mechanisms and the structure of active catalytic species. For example, in two cases of Sharpless epoxidation of allylic alcohols, they found that the parameters determined from a fit to their ML_2 model were in agreement with experimental evidence, indicating the presence of a more abundant but less reactive dimeric *meso* complex.

As in any such modeling exercise, an independent experimental corroboration of the mathematical fit is desirable in order to test the model and to validate the physical significance of the values obtained for the model parameters. The purpose of this paper is to demonstrate that an independent test of the models developed by Kagan and co-workers may readily be carried out by combining the observed enantioselectivity data with measurements of the overall rate of the catalytic reaction carried out at different levels of catalyst enantiomeric excess. In addition, it is shown that consideration of reaction rate behavior combined with enantioselectivity can provide further mechanistic insights and aid in the development of efficient synthetic strategies for asymmetric catalytic reactions using nonenantiopure catalysts.

Background

If partially resolved chiral ligands are used to prepare an organometallic catalyst system containing two or more ligands, there exists the possibility of forming achiral and heterochiral complexes in addition to homochiral catalytic species. The models developed by Kagan and co-workers[1a,b] show how the ultimate enantioselectivity observed in a reaction carried out using such a mixture of catalysts will depend on the relative concentrations and reactivities of each catalytic species in the mixture, as well as on the intrinsic product enantioselectivity obtained with each catalyst in the asymmetric reaction. A plot of reaction product enantioselectivity (ee_{prod}) as a function of enantiomeric excess of the catalyst (ee_{aux}) reveals whether a nonlinear relationship exists. The mathematical models may then be used to fit experimental data points to an equation containing a number of adjustable parameters related to the catalyst properties.

Each experimental data pair (ee_{aux}, ee_{prod}) corresponds to the result of one catalytic reaction using a chiral catalyst or auxiliary of a different level of enantiomeric excess. Thus the number of data pairs available for the curve fitting is usually small (most published examples of nonlinear effects report fewer than 10 different enantiomeric excesses for a given catalyst−ligand system), and the simplest of the reported mathematical models contains two adjustable parameters. The most statistically and physically meaningful results from such multiparameter model fits are obtained when the number of data points far exceeds the number of adjustable parameters in the model, or when an independent corroboration of the values of the parameters may be obtained. It is shown in this paper that the mathematical models developed by Kagan and co-workers may be used to predict overall reaction rate in addition to enantioselectivity. The simplest ML_2 model of Kagan and co-workers is used here to illustrate how experimental reaction rate measurements thus may give an independent confirmation of the physical significance of the conclusions reached from application of the model to experimental enantioselectivity data. Simulations based on

* E-mail: blackmond@mpi-muelheim.mpg.de.

⊗ Abstract published in *Advance ACS Abstracts,* December 15, 1997.

(1) (a) Guillaneux, D.; Zhao, S. H.; Samuel, O.; Rainford, D.; Kagan, H. B. *J. Am. Chem. Soc.* **1994**, *116*, 9430−39. (b) Puchot, C.; Samuel, O.; Duñach, E.; Zhao, S.; Agami, C.; Kagan, H. B. *J. Am. Chem. Soc.* **1986**, *108*, 2353−57. (c) Oguni, N.; Matsuda, Y.; Kaneko, T. *J. Am. Chem. Soc.* **1988**, *110*, 7877. (d) Noyori, R.; Kitamura, M. *Angew. Chem., Int. Ed. Engl.* **1991**, *30*, 49−69. (e) Kitamura, M.; Suga, S.; Niwa, M.; Noyori, R. *J. Am. Chem. Soc.* **1995**, *117*, 4832−4842. (f) Bolm, C. *Tetrahedron: Asymmetry* **1991**, *2*, 701−704. (g) Mikami, K.; Motoyama, Y.; Terada, M. *J. Am. Chem. Soc.* **1988**, *116*, 2812−2820. (h) Mikami, K.; Matsukawa T. *Tetrahedron* **1992**, *48*, 5671−80. (i) Keck, G. E.; Krishnamurthy, D.; Grier, M. C. *J. Org. Chem.* **1993**, *58*, 6543−6544.

(2) See also these reviews: (a) Kagan, J. B.; Girard, C.; Guillaneux, D.; Rainford, D.; Samuel, O.; Zhand, S. Y.; Zhao, S. H. *Acta Chem. Scand.* **1996**, *30*, 345−352. (b) Bolm, C. In *Advanced Asymmetric Synthesis*; Stephenson, G. R., Ed.; Blackie A&P: Glasgow, 1996; pp 9−26.

S0002-7863(97)03049-7 CCC: $14.00

Scheme 1

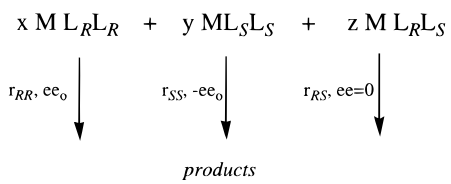

$$K = \frac{z^2}{xy}$$

$$\beta = \frac{z}{x+y}$$

$$g = \frac{r_{RS}}{r_{RR}}$$

$$r_{RR} = r_{SS}$$

$$ee_{aux} = \frac{\sum L_R - \sum L_S}{\sum L_R + \sum L_S} = \frac{[2x+z]-[2y+z]}{[2x+z]+[2y+z]} = \frac{x-y}{x+y+z} = x-y$$

the more complicated ML_3 system are then carried out to provide an additional vivid illustration of the implications of reaction rate in assessing the overall synthetic efficiency, in comparison to the chiral efficiency, of nonenantiopure catalyst systems.

Results and Discussion

ML_2 Model. Scheme 1 shows the reaction network for the ML_2 model developed by Kagan and co-workers[1a,b] for asymmetric catalysis based on the fast ligand exchange between two chiral ligands, L_R and L_S, and a metal center M. The model assumes that at any given level of catalyst enantiomeric excess (that is, at fixed amounts of L_R and L_S), a steady-state exists for the concentrations of the three catalyst species in the mixture, two homochiral complexes ML_RL_R, ML_SL_S, and a *meso* complex ML_RL_S, in the respective relative concentrations *x*, *y*, and *z*. When the ligand distribution is equal to the equilibrium distribution (Curtin−Hammett limit of fast ligand exchange), the parameter *K* becomes the equilibrium constant. The catalytic reaction carried out using these complexes is assumed to be pseudo-zero-order in substrate and first order in catalyst concentration. For a reaction carried out with either of the enantiopure catalysts ML_RL_R or ML_SL_S, the reaction rate is identical ($r_{RR} = r_{SS}$) and the product enantioselectivities are opposite (ee_o and $-ee_o$, respectively). Racemic product is formed from the *meso* catalyst which exhibits the relative reactivity equal to the parameter *g*. With these assumptions, and with the enantiomeric excess of the chiral catalyst expressed as ee_{aux}, Kagan and co-workers showed that the enantioselectivity of the reaction products ee_{prod} obtained from this mixture of catalysts will vary with ee_{aux} according to

$$ee_{prod} = ee_o ee_{aux}[(1+\beta)/(1+g\beta)] \qquad (1)$$

The ratio of *meso* to chiral complexes is given by the parameter β, which was shown in ref 1 to be related to *K* and ee_{aux} according to

$$\beta = \frac{z}{x+y} = \frac{-Kee_{aux}^2 + \sqrt{-4Kee_{aux}^2 + K(4 + Kee_{aux}^2)}}{4 + Kee_{aux}^2} \qquad (2)$$

The value for β varies with ee_{aux} because the relative amounts of the three catalysts (*x*, *y*, and *z*) vary with catalyst enantiomeric excess, but the value of the equilibrium constant *K* is fixed for a given metal−ligand system at a given temperature. Equations 1 and 2 may be fit to a series of experimental data pairs of (ee_{aux}, ee_{prod}) to obtain values for *K* and *g*. The values for these two parameters provide the basis for discussions of the mechanistic implications of the model in a particular application. For example, large values of *K* indicate predominance of the *meso* species, and values of *g* less than one mean that the *meso* species is less reactive than the enantiopure catalyst.

Table 1. Relative Concentrations of Catalyst Species Complexes ML_RL_R (*x*), ML_SL_S (*y*), and ML_RL_S (*z*) at Each Level of Catalyst Enantiomeric Excess (ee_{aux})[a]

ee_{prod}	ee_{aux}	*x*	*y*	*z*
0	0	0.030	0.030	0.940
0.23	0.1	0.107	0.007	0.886
0.42	0.2	0.203	0.003	0.794
0.47	0.3	0.301	0.002	0.697
0.71	0.5	0.500	0.001	0.499
0.76	0.65	0.65	<0.001	0.35
0.87	0.85	0.85	<0.001	0.15
0.95	1	1	0	0

[a] Values are for the example in ref 1a of the Sharpless epoxidation of geraniol carried out using (Ti(O-i-Pr)$_4$/(*R*,*R*)-DET) with different levels of enantiomeric excess of the tartrate. The relative concentrations *x*, *y*, and *z* are determined as described above from the ML_2 model fit to experimental (ee_{aux}, ee_{prod}) data pairs using the parameters $K = 1000$ and $g = 0.35$. The experimental ee_{prod} and ee_{aux} are experimental values taken from ref 1a, Figure 5a.

Kagan and co-workers report their model results in terms of these parameters *K* and *g*; it will be shown here how the model may also be used to determine the separate relative concentrations of the three catalyst species ML_RL_R, ML_SL_S, and ML_RL_S (respectively *x*, *y*, and *z*) and how these concentrations may be used in turn to determine the reaction rate predicted by the model at each level of catalyst enantiomeric excess.

The sum of the relative concentrations *x*, *y*, and *z* of the different catalyst species in the different branches of the network must add up to 1 ($x + y + z = 1$). This relationship coupled with the definitions of *K* and β given above and in Scheme 1 provide three independent equations from which the individual values of *x*, *y*, and *z* may be determined at any value of ee_{aux}.

The overall reaction rate for the network in Scheme 1 is given by the summation of the rates of reaction of each pathway. With the assumptions of the ML_2 model given above, this rate will be given by eq 3. The reaction rate will be different for reactions carried out with catalysts of different enantiomeric excess because *x*, *y*, and *z* are each a function of ee_{aux}.

$$r_{total} = xr_{RR} + yr_{RR} + gzr_{RR} = (x + y + gz)r_{RR} \qquad (3)$$

Just as the model allows plots of ee_{prod} vs ee_{aux} to be drawn, similar plots of r_{total} vs ee_{aux} may be constructed to show the model prediction of the overall rate at each level of enantiomeric excess of the catalyst or auxiliary used to effect the asymmetric reaction. If the rate for the reaction carried out using an enantiopure catalyst or auxiliary is measured, then the value of r_{RR} is known. If this rate is not known, the rate of reaction at each value of catalyst enantiomeric excess may be normalized to the unknown value of r_{RR}.

As an illustration we consider the ML_2 model fit to experimental data described by Kagan and co-workers[1a] for geraniol epoxidation using the Sharpless reagent (Ti(O-i-Pr)$_4$/(*R*,*R*)-DET) with different levels of enantiomeric excess of diethyl tartrate (DET). The experimental data points and the model fit of ee_{prod} vs ee_{aux} are reproduced here as Figure 1a ($K = 1000$ and $g = 0.35$).[3] The difference between the data and the dashed line shows the deviation from linearity of the system.

Table 1 shows the calculated relative concentrations of the three catalyst species as a function of ee_{aux} determined from

(3) Figure 1a in this paper reproduces the model fit given in Figure 5a of ref 1a.

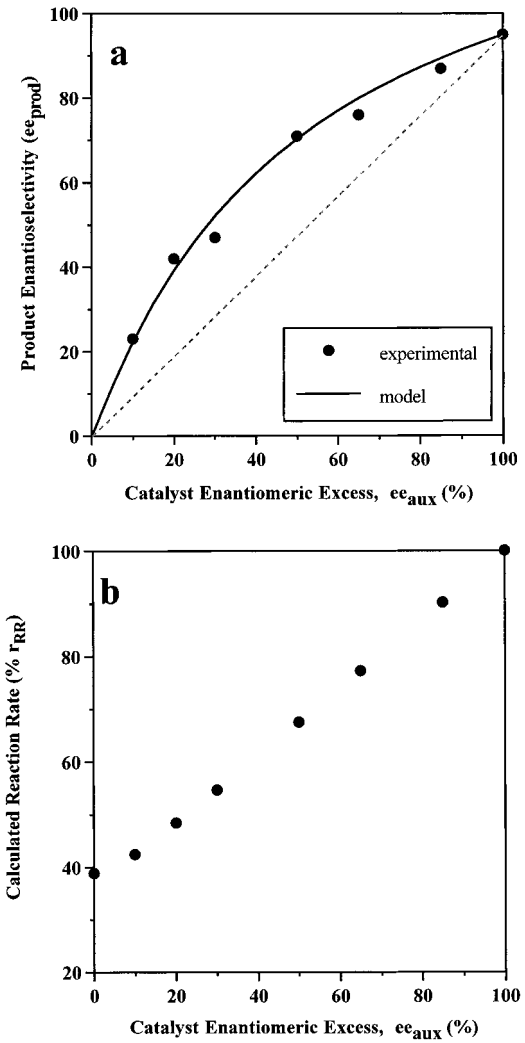

Figure 1. (a) Relationship between product enantioselectivity and catalyst enantiomeric excess and (b) model prediction of the overall reaction rate for each (ee_{aux}, ee_{prod}) data pair shown in part a. (Part a: Reprinted from ref 1a, Figure 5a. Copyright 1994 American Chemical Society.)

this model as described above. Figure 1b shows the predicted overall rate from eq 3 for each value of ee_{aux}. Thus, if experimental reaction rate measurements for the reactions described by these (ee_{aux}, ee_{prod}) data were available, comparison of the experimental data to the predictions in Figure 1b would provide a test of the physical significance of the model-derived parameters. Agreement between experimentally measured and model-predicted reaction rates would confirm the applicability of the model as a physical description of the nonlinear catalyst behavior. Conversely, a discrepancy between the two would suggest that one or more of the assumptions used in building the model are not applicable to the catalytic system in question.

In the case where experimental rate measurements are not in agreement with the model predictions, an opportunity for further mechanistic insight is offered by examination of the model's underlying assumptions. For example, the model requires fast initial metal−ligand equilibration; if this assumption is not met then the value of *K* may not remain constant as ee_{aux} is varied, and a single model-derived value of this constant would not be physically meaningful. Such a case might offer clues about metal−ligand binding and dissociation rates in comparison to the catalytic reaction rate which could then be used to optimize ligand design.

The model also assumes that no free ligand remains in solution after this metal−ligand exchange equilibrium is reached and that no further changes to the catalyst species occur during the catalytic reaction, such as the formation of new metal−ligand species through binding of the reaction product. Reaction rate measurements might thus help to identify cases in which product inhibition, autocatalysis, or other phenomena occur in which the active catalyst species are modified as the reaction progresses.

Another case where reaction rate data might be useful would be in distinguishing between a catalyst system following an ML_n model such as is considered here and one corresponding to a "reservoir model", the second type of model developed by Kagan and co-workers.[1a,b] In this model, inactive mixed-ligand complexes are formed which may alter the relative percentages of the remaining *R* and *S* ligands from which the active catalysts are formed; this may alter the enantiomeric excess of the remaining species actively engaged in catalysis. When the achiral or heterochiral species in ML_n systems have low activity, these two models may give similar predictions for enantioselectivity. The goodness of fit of experimental rate data to the prediction for each model might help in choosing which offers a closer description of the system under study.

Another important assumption of the ML_n models is that the reaction rate is zero order in substrate for all catalytic species participating in the network. When different catalytic species participating in the same reaction exhibit different rate laws, enantioselectivity can vary over the course of the reaction as a function of conversion of substrate. In such a case, product enantioselectivity observed at the reaction endpoint would be a function of the initial substrate concentration. The features of a plot of ee_{prod} vs ee_{aux} would thus depend on the initial substrate concentration chosen for the series of experiments, and neither rate nor enantioselectivity behavior would be accurately described by an ML_n model.

In cases where the applicability of the model is indeed confirmed by agreement between experimental and model-derived reaction rate data, the calculations described above can provide further insights into the physical implications for catalyst systems which are found to follow this model. Kagan and co-workers report their ML_2 model results in terms of the parameters *K* and *g*, but it is interesting to consider what the values of these parameters signify for the separate relative concentrations of the three catalyst species predicted by the model. Table 1 shows that the ML_SL_S catalyst concentration is close to zero at all levels of catalyst enantiomeric excess for the *K* and *g* values determined from the model fit. Therefore the catalyst mixture consists primarily of only two catalytic species, the enantiopure ML_RL_R and the *meso* ML_RL_S complexes. This result is predicted for high values of the equilibrium constant, *K*, indicating that the *meso* complex has formed at the expense of *all* of the minor enantiomeric ligand L_S which was originally present in the mixture. The reaction is therefore catalyzed by a mixture of the ML_RL_R catalyst giving product of ee_o, and the *meso* ML_RL_S species which gives racemic product. The observed enantioselectivity will reflect some dilution of ee_o by the racemic product formed by the *meso* complex, but since none of the pure ML_SL_S complex remains to contribute its opposite enantioselectivity $-ee_o$, the ultimate effect will be a positive deviation from the linear relationship between ee_{prod} and ee_{aux}, since the reaction rate of the *meso* complex is less than that of the enantiopure catalyst ($r_{RS} = 0.35r_{RR}$).[4]

(4) This concept of the selective sacrifice of one chiral ligand is also discussed in the second model presented by Kagan and co-workers, which describes how the existence of a reservoir of inactive species outside the catalytic cycle may serve to increase the enantiopurity of the catalytic species inside the cycle. They have also discussed how the reservoir model may be used in conjunction with the ML_x models.

Figure 1b makes it clear, however, that the cost of this amplification of product chirality comes in the form of a lower overall reaction rate. Formation of the *meso* complex is an effective method of engaging all of the L_S ligand and therefore suppressing the opposite chemistry of the enantiopure ML_SL_S catalyst. However, this necessarily also sacrifices some of the L_R ligand, decreasing the total concentration of the ML_RL_R species, which is the catalyst responsible for high activity and selectivity. For example, Figure 1a,b shows that a catalyst of only 20% ee_{aux} yields a reaction product of double this enantioselectivity, but at a reaction rate equal to only half that of the enantiopure catalyst.

Other examples of even more dramatic positive asymmetric amplification in the ML_2 system have been shown in theoretical curves by Kagan and co-workers, corresponding to the case of complete monopolization of the minor ligand by an even less reactive *meso* species (higher K values, lower g values) than in the example just shown. The penalty in reaction rate for chiral amplification will be even greater in such a case. For example, the model predicts that product enantioselectivities approaching 90% may be obtained with chiral catalysts of only 10% purity (model parameters $K = 2500$, $g < 0.01$), but the overall reaction rate in this catalyst mixture will be ten times slower than that of the enantiopure catalyst. Thus the chiral amplification in this model may be thought of as an advantageous selective poisoning of the active catalyst: the stronger the positive chiral amplification is, the lower the absolute concentration of active catalyst ML_RL_R in the catalyst mixture.[5] This rate behavior has implications for the practical exploitation of nonenantiopure catalyst systems in organic synthesis. The advantage of combining some form of ligand-accelerated catalysis with the use of such nonenantiopure systems also becomes apparent.[6,7] An amplified rate of the reaction by some modifier added to the system described here would help to offset the effects of the decreased concentration of the ML_RL_R catalyst in the catalytic cycle.

Although most studies of asymmetric catalytic reactions report final conversion of substrate or isolated product yield in addition to enantioselectivity, kinetic measurements of substrate conversion as a function of reaction time are carried out less often. Noyori and co-workers[1e] have completed some of the most extensive kinetic studies as well as detailed spectroscopic and structural investigations of nonlinear effects in their work on the alkylation of aldehydes by dialkylzincs catalyzed by chiral β-dialkylamino alcohols. Their studies include consideration of the consequences for reaction rate of the phenomena which lead to nonlinear enantioselectivity behavior. Although that system cannot be described by a simple ML_2 model, the reaction exhibits an overall rate decrease with decreasing ee_{aux} for reasons similar to those discussed here. Potential catalytic species which become engaged in mixed-ligand complexes alter the overall observed catalytic behavior because these complexes exhibit different activity and enantioselectivity and effectively cause a change the overall enantiomeric excess of the species remaining in the catalytic cycle. Our calculations also show that consideration of reaction rate as well as enantioselectivity provides a more complete picture of catalyst behavior in asymmetric catalytic reactions.

Scheme 2

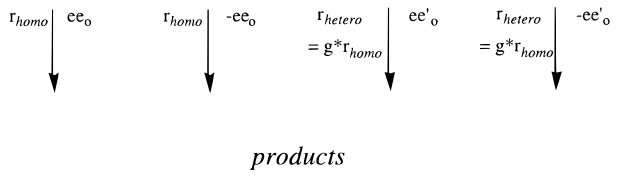

ML_3 Model. An even more striking example of the implications of reaction rate behavior for synthetic efficiency may be found by considering the ML_3 model described by Kagan and co-workers.[1a,b] This model, shown in Scheme 2, treats the theoretical case where one metal center and three chiral ligands participate in the catalytic event. In the simplest case,[8] this gives four catalytic species, two homochiral species and two heterochiral species. These heterochiral species, in contrast to the *meso* species found in the ML_2 system, are chiral and yield a chiral product in the catalytic reaction.

Kagan and co-workers[1a] carried out simulations of the enantioselectivity behavior of the ML_3 system as a function of catalyst enantiomeric excess, assuming that a statistical distribution of the chiral ligands exists between these four complexes ($K = 3$). As an illustration, they treated the case where the homochiral complexes give an enantiopure product ($ee_o = 100\%$) and the heterochiral complexes give $ee'_o = 50\%$. The relative reactivity of the heterochiral complexes was varied from zero ($g = 0$) to 2 orders of magnitude greater than that of the homochiral complexes ($g = 100$). Figure 2 reproduces their simulation for these two extremes of relative reactivity of the pure and mixed-ligand complexes showing how product enantioselectivity varies with ee_{aux}. Significant deviations from linear behavior are observed in this theoretical example. It is clear that high values of g (a highly reactive heterochiral complex) lead to a strong negative nonlinear effect; a catalyst of 50% enantiomeric excess gives a product of only 26% enantioselectivity. In a system where g equals zero (inactive heterochiral complexes), by contrast, the product enantioselectivity is strongly amplified: 93% ee_{prod} is achieved at 50% ee_{aux}. Thus, for an ML_3 system with these characteristics, it would appear that a strategy for high chiral efficiency would be favored by an inactive heterochiral complex.

Analogous to the calculations presented here for the ML_2 system, we may now determine how both the relative concentrations of the catalytic species and the reaction rate in the ML_3 system vary as the relative amounts of L_R and L_S (ee_{aux}) are varied.[9] Figure 3 shows the relative concentrations of the catalyst species in the ML_3 system for the case of a statistical distribution of ligands ($K = 3$). Measurable concentrations of all four complexes are present until ee_{aux} reaches ~70%. Thus in the case of a low K value, the heterochiral complexes have

(5) For reports on chiral poisoning, see: (a) Alcock, N. W.; Brown, J. M.; Maddox, P. J. *J. Chem. Soc., Chem. Commun.* **1986**, 1532−33. (b) Maruoka, K.; Yamamoto, H. *J. Am. Chem. Soc.* **1989**, *115*, 789−90. (c) Faller, J. W.; Parr, J. *J. Am. Chem. Soc.* **1993**, *115*, 804−05. Kagan and co-workers have also pointed out how the concept of chiral poisoning increases the concentration of enantiopure catalyst within the catalytic cycle.

(6) (a) Jacobsen, E. N.; Marko, I.; France, M. B.; Svendsen, J. S.; Sharpless, K. B. *J. Am. Chem. Soc.* **1989**, *111*, 737−739. (b) Berrisford, D. J.; Bolm, C.; Sharpless, K. B. *Angew. Chem.* **1995**, *34*, 1059−1070.

(7) A related idea described recently is called "chiral activation". Addition of a species which selectively interacts with one enantiomer in a racemic catalyst mixture resulted in a significant rate acceleration of the reaction carried out by the activated catalyst species. No "sacrifice" of either catalytic species occurs in this case; in fact, the remaining, unactivated enantiomer continues to react with its intrinsic activity and (opposite) enantioselectivity: (a) Mikami, K.; Matsukawa T. *Nature* **1997**, *385*, 613−15. (b) Matsukawa, T.; Mikami, K. *Tetrahedron*: *Asymmetry* **1997**, *8*, 815−816.

(8) The actual case of an ML_3 catalyst is probably more complex than that described by this model. The two heterochiral complexes, $ML_RL_RL_S$ and $ML_SL_SL_R$ would most likely be further differentiated by their relative positions in the coordination sphere of the metal: for example, in an octahedral complex, the intrinsic enantioselectivities of catalysts containing homochiral ligands *cis* to one another could be different than that of a complex where heterochiral ligands are in a *cis* configuration.

(9) Details on these calculations are available in the Supporting Information.

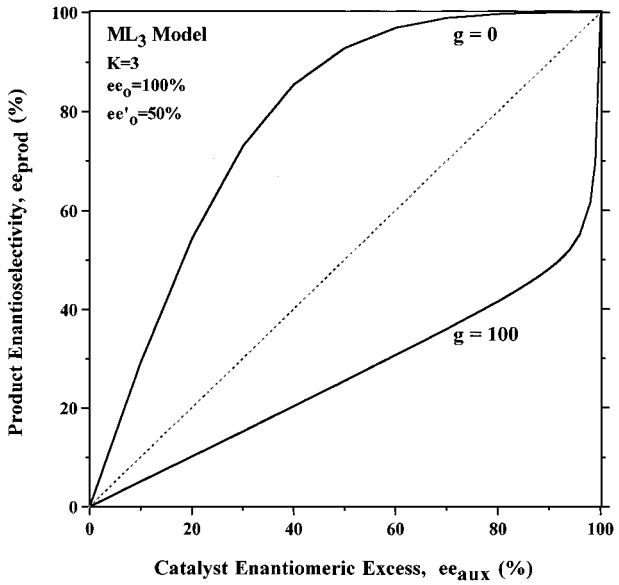

Figure 2. Calculation of the nonlinear relationship between product enantioselectivity and catalyst enantiomeric excess for the ML_3 model, reproduced from Ref. 1a, Figure 9 (Copyright 1994 American Chemical Society), with the following parameters: $K = 3$; enantioselectivity from homochiral species $ee_o = 100\%$; enantioselectivity from heterochiral species $ee'_o = 50\%$; relative reaction rate for heterochiral vs homochiral species, $g = 0$ or $g = 100$. The dashed line shows the linear relationship.

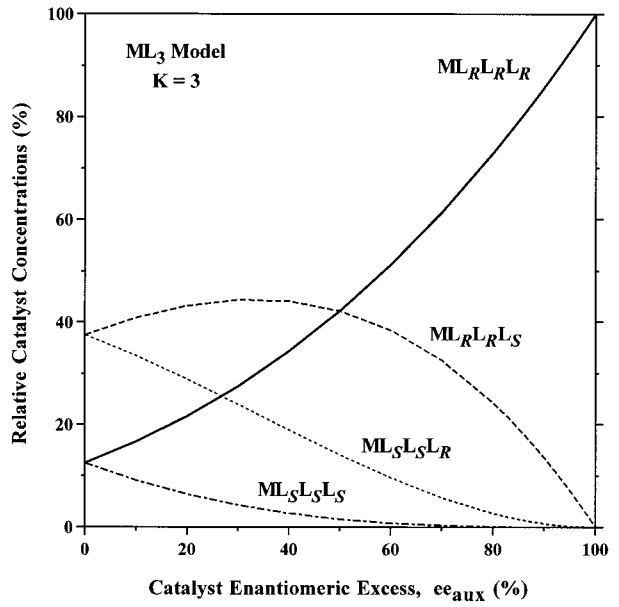

Figure 3. Relative concentrations of the four catalyst species present in the ML_3 system as a function of catalyst enantiomeric excess, for the case of a statistical distibution of L_R and L_S ligands ($K = 3$).

not completely engaged all of the minor ligand L_S, in contrast to the observation in the previous ML_2 system where $K = 1000$. As ee_{aux} increases from 0 to 100% (and consequently the percentage of L_R increases from 50% to 100%), the concentration of the homochiral $ML_RL_RL_R$ increases steadily. The heterocomplex $ML_RL_RL_S$ at first shows an increase in concentration as ee_{aux} increases. The concentrations of this complex and the other two L_S-containing complexes ($ML_SL_SL_R$ and $ML_SL_SL_S$) eventually decrease to zero as ee_{aux} approaches 100% and the L_S concentration in the system approaches zero. The relative concentrations of these complexes are fixed by the value of the equilibrium constant K and are not affected by parameters of the catalytic reaction. Thus Figure 3 describes how the relative amounts of the different catalyst species vary with ee_{aux}

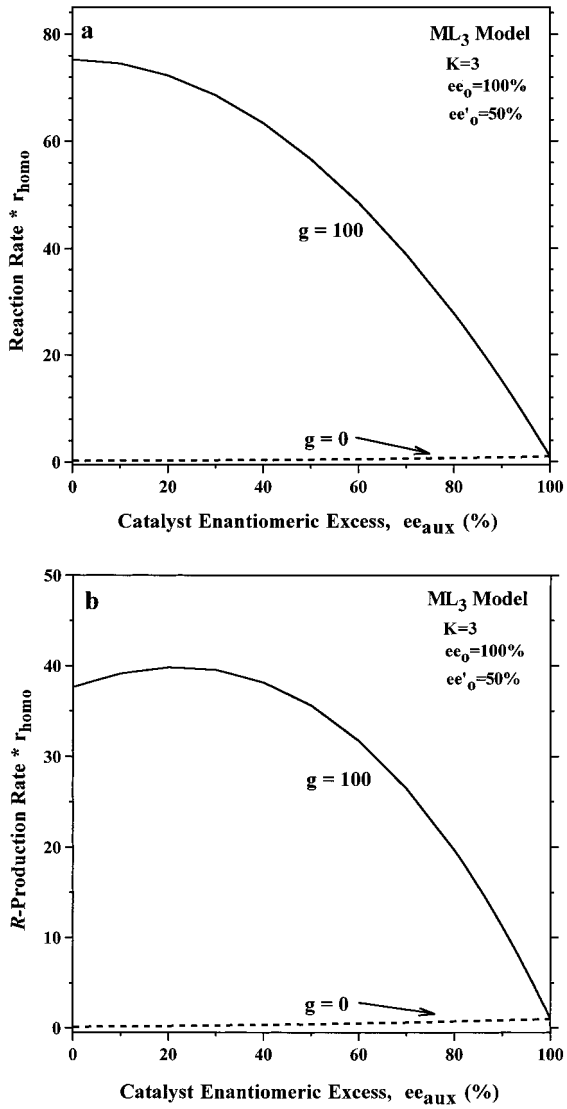

Figure 4. Reaction rate as a function of catalyst enantiomeric excess in the ML_3 system: (a) overall reaction rate and (b) rate of production of the *R* product. Parameters: $K = 3$; enantioselectivity from homochiral species, $ee_o = 100\%$; enantioselectivity from heterochiral species $ee'_o = 50\%$; relative reaction rate for heterochiral vs homochiral species, $g = 0$ or $g = 100$.

regardless of the intrinsic enantioselectivities or relative reactivities (ee_o, ee'_o, and g) of the catalytic reaction in which these species participate.

Also analogous to our calculations for the ML_2 system, determination of the relative catalyst concentrations allows us to explore reaction rate behavior at different ee_{aux} values for the ML_3 system shown in Figure 3.[9] For this illustration, we take the two cases $g = 0$ and $g = 100$ from Figure 2 ($ee_o = 100\%$, $ee'_o = 50\%$). Figure 4 shows the model prediction of reaction rate vs ee_{aux} for these two cases.

The reaction rate data in Figure 4a reveal a striking contrast to the conclusions reached from the enantioselectivity plot for the same two cases shown in Figure 2. The system which exhibited a strong *negative* nonlinear effect in enantioselectivity shows a strong *positive* amplification in reaction rate. At low values of ee_{aux}, the reaction rate for the case where $g = 100$ is 2 orders of magnitude faster than that for $g = 0$ as well as that found for the linear case (r_{homo}). This rate difference decreases as ee_{aux} increases, but a 10-fold difference in rates remains even at $ee_{aux} = 95\%$. Thus it is demonstrated for the ML_3 case how high asymmetric amplification in product chirality is achieved

at an even more dramatic cost in reaction rate than was observed in the ML_2 model.

We may put this difference in rates in terms of the overall synthetic efficiency of the reaction by considering specifically the rate of production of the desired *R* product. Figure 4b compares the *R* product rate for the cases of $g = 0$ and $g = 100$ shown in 4a. This shows that at $ee_{aux} = 50\%$, while the catalyst mixture exhibits a nearly 4-fold *positive* amplification in product enantioselectivity in the case where $g = 0$ compared to $g = 100$, in fact it produces 100 times *less R* product molecules in a given reaction time. Thus, a significant *absolute amplification* in the *R* product as a function of ee_{aux} is observed for the case which exhibits a *negative* nonlinear relationship between ee_{prod} and ee_{aux}. It should be emphasized that this *R* product rate is also amplified over the rate which would be observed in the absence of a nonlinear effect in ee_{aux}.

The result that a catalyst mixture with poorer enantioselectivity gives a higher synthetic efficiency to the desired product may appear to be counterintuitive, but this conclusion is easily rationalized by recalling that selectivity in any reaction is given by a *ratio* of reaction rates. The individual product formation rates may rise or fall as selectivity changes. The overall synthetic yield in a reaction will depend both on how selectively and on how fast a product is formed. Thus a strategy for efficient catalytic synthesis of chiral compounds should take into account both enantioselectivity (chiral efficiency) and reaction rate (overall synthetic efficiency) behavior in the choice of a catalyst system to carry out the reaction. For cases where separation of the two enantiomeric reaction products is very difficult or very costly, a penalty in the form of severely suppressed production rates may ultimately be an acceptable price to pay for high enantioselectivity in the catalytic reaction.

Conclusions

This paper highlights the importance of considering reaction rate data in conjunction with enantioselectivity results for asymmetric catalytic reactions. It is demonstrated how kinetic measurements may provide an independent means of confirming parameters derived from theoretical models such as those developed by Kagan and co-workers.[1a,b] Thus reaction rate data may help to corroborate the insights that these models offer about the participation of different catalyst species in the reaction mechanism. Alternatively, experimental rate data may point out cases where the models fail to provide an adequate physical description of the catalytic system.

An example is given to illustrate that a *negative* nonlinear effect in enantioselectivity may be accompanied by a significant *positive* amplification in reaction rate. This work illustrates how consideration of reaction rates can add valuable insights for developing synthetic strategies for the efficient production of chiral compounds from nonenantiopure catalyst mixtures. Understanding the kinetic aspects of these reactions may thus help lead to a fuller understanding and ultimate exploitation of nonlinear effects in asymmetric catalysis.

Supporting Information Available: Calculations of relative concentrations of catalytic species (*x*, *y*, *z*, and *w*) and the reaction rate for the ML_3 model (2 pages). See any current masthead page for ordering and Internet access instructions.

JA973049M